

Bulk-plasmon dispersion relations in metals

Ll. Serra, F. Garcias, and M. Barranco*

Departament de Física, Universitat de les Illes Balears, E-07071 Ciutat de Mallorca, Spain

N. Barberán*

School of Physics, University of East Anglia, Norwich NR4 7TJ, United Kingdom

J. Navarro

*Departament de Física Atòmica, Molecular i Nuclear and IFIC (Consejo Superior de Investigaciones Científicas),
Universitat de Valencia, E-46100 Burjassot, Spain*

(Received 26 July 1990; revised manuscript received 22 January 1991)

Using an extended-random-phase-approximation sum-rule technique, we have investigated the bulk-plasmon dispersion relation, incorporating in a simple way exchange and correlation effects within the jellium model. The results obtained are compared with recent experimental findings. The key role played by exchange and correlation effects in improving the agreement between theory and experiment is stressed. The static polarizability has also been calculated as a function of q . The formulas can be easily modified to incorporate band-structure effects (through an intraband electron effective mass) and core-polarization effects (through a static dielectric constant).

I. INTRODUCTION

Recently, high-resolution electron-energy-loss spectroscopy (EELS) experimental results of the bulk-plasmon dispersion relation in aluminum¹ and alkali metals² have been reported. These accurate measurements have been used by the authors of Refs. 1 and 2 (thereafter referred to as SFF) to discuss the shortcomings of different theoretical approaches aimed at describing the bulk plasmon, in particular the apparent inability of the random-phase approximation (RPA) to reproduce their findings. In this work we will show that the extended RPA (ERPA), which results when exchange and correlation effects are taken into account, is able to fairly reproduce the bulk-plasmon dispersion relation for high-density nearly-free-electron (NFE) metals, whereas it fails to reproduce the experimental results for low-density NFE metals like Cs.

The method we have used has been described in detail in Refs. 3–5 and references therein. It is based on the evaluation of a few ERPA sum rules m_k , defined as

$$m_k \equiv \sum_n \epsilon_n^k |\langle n | Q | \phi \rangle|^2,$$

where the sum extends over all the excited states. Q is the operator causing the excitation of the system, and ϵ_n , $|n\rangle$, and $|\phi\rangle$ are, respectively, the excitation energies, the excited states, and the ground state (g.s.) of the system.

Defining the average energies $E_k \equiv (m_k/m_{k-2})^{1/2}$, it can be shown that the mean excitation energy $\bar{E} = m_1/m_0$ is bounded as $E_1 \leq \bar{E} \leq E_3$. The usefulness of this inequality lies in the fact that m_1 and m_3 (thus E_3) can be obtained with ERPA accuracy, while there are arguments to infer that m_{-1} ERPA (thus E_1) can be estimated with some accuracy from constrained Thomas-

Fermi⁶ (TF) and hydrodynamical (HD) calculations.^{7–9}

If a collective state exhausts most of the strength corresponding to a given excitation operator Q , E_3 and E_1 are close and any of them can be taken as an estimate of \bar{E} . In actual physical situations, it is not always simple to identify the operator causing the excitation, and one has to resort to physically reasonable choices, like multipole operators of the kind $r^L Y_{L0}$ and $j_L(qr) Y_{L0}$, where $j_L(qr)$ is a spherical Bessel function and Y_{L0} a spherical harmonic, or plane-wave, operator $e^{iq \cdot r}$. It may well happen that E_1 and E_3 are rather different for a state whose collectivity is well established experimentally, this being an indication of the inability of the chosen operator to test the collective character of that state. As we shall indicate below, E_1 and E_3 embody different physics, so it is also possible that E_1 or E_3 corresponds to the right description of a physical phenomenon, but not both.

This paper is organized as follows. In Sec. II we obtain the E_1 and E_3 average energies corresponding to a plane-wave operator in the jellium approximation. These energies are compared with the experimental results of SFF in Sec. III. Finally, we draw our conclusions in Sec. IV.

II. THE E_1 AND E_3 AVERAGE ENERGIES FOR A PLANE-WAVE OPERATOR

For EELS in bulk materials, the plane wave is the most natural operator to describe the collective excitations of the material. Within the jellium model, it is straightforward to obtain m_{-1} , m_1 , and m_3 . We shall consider an electron Hamiltonian density consisting of a kinetic term, a Coulomb direct term, a Coulomb exchange term of Slater type:

$$\epsilon_{\text{ex}} = -\frac{3}{4} \left[\frac{3}{\pi} \right]^{1/3} n_0^{4/3}, \quad (1)$$

and a correlation term of Wigner type:

$$\epsilon_{\text{cor}} = -\frac{an_0}{b+r_s}, \quad (2)$$

where n_0 is the electron density, $r_s = [3/(4\pi n_0)]^{1/3}$ is the bulk radius per electron, $a = 0.44$ and $b = 7.8$. We shall use atomic units (a.u.) throughout.

The sum rules m_1 and m_3 can be obtained from

$$\begin{aligned} m_1 &= \frac{1}{2} \langle \phi | [Q^+, [H, Q]] | \phi \rangle, \\ m_3 &= \frac{1}{2} \langle \phi | [[Q^+, H], [H, [H, Q]]] | \phi \rangle, \end{aligned} \quad (3)$$

where Q is the plane-wave one-body operator, $Q = \sum_k \exp(i\mathbf{q} \cdot \mathbf{r}_k)$, and H is the Hamiltonian of the electron system. m_1 and m_3 can be evaluated either directly from Eqs. (3), or scaling the g.s. wave function, as explained in Refs. 3, 5, and 10. The final expressions for these sum rules per electron are

$$\begin{aligned} \frac{m_1}{N} &= \frac{q^2}{2}, \\ \frac{m_3}{N} &= \frac{q^2}{2} \left[\omega_p^2 + \left(\frac{3}{5} v_F^2 - \frac{v_F}{3\pi} - \xi \right) q^2 + \frac{1}{4} q^4 \right], \end{aligned} \quad (4)$$

where

$$\xi = -n_0 \frac{\partial^2 \epsilon_{\text{cor}}}{\partial n_0^2} = \frac{2a}{9} r_s \frac{b + 2r_s}{(b + r_s)^3}. \quad (5)$$

In these formulas, $\omega_p = (3/r_s^3)^{1/2}$ is the plasma frequency and $v_F = (3\pi^2 n_0)^{1/3}$ the Fermi velocity. Thus, we obtain for the E_3 energy:

$$\begin{aligned} E_3^2 &\equiv \frac{m_3}{m_1} = \omega_p^2 + \left(\frac{3}{5} v_F^2 - \frac{v_F}{3\pi} - \xi \right) q^2 + \frac{1}{4} q^4 \\ &\equiv \omega_p^2 + \alpha_3 q^2 + \frac{1}{4} q^4. \end{aligned} \quad (6)$$

This expression, hereafter referred to as the elastic dispersion relation, has been deduced in Ref. 5 using the spherical Bessel functions expansion of $e^{i\mathbf{q} \cdot \mathbf{r}}$ and considering the limit of a large sphere of constant density n_0 . The q^2 term in Eq. (6) has three contributions. The $3v_F^2/5$ contribution has a kinetic-energy origin, and is the only one that appears in what is called the RPA coefficient.⁸ The $v_F/3\pi$ contribution comes from the exchange interaction and the ξ term from the correlation energy; it is smaller than the exchange contribution. The q^4 term also comes from the kinetic energy; it is the quasifree-electron kinetic-energy contribution.⁵ Equations similar to our Eqs. (4) were also obtained in Ref. 11, although the exchange and correlation contributions were not given in an explicit form.

Equation (6) is an *exact* ERPA result involving no q^2 expansion. It is valid for *any* q , even above the cutoff value $q_c = \omega_p/v_F$. The only assumptions made to arrive at it are (i) the operator $e^{i\mathbf{q} \cdot \mathbf{r}}$ causes the bulk excitations of the infinite system; (ii) the positive charge background is described within the jellium model; and (iii) exchange and correlation effects in the electron-electron interaction

are described in a local-density approximation (LDA). Actually, it is due to the use of the LDA for the exchange-correlation energy that there are no exchange-correlation contributions of order higher than q^2 . To avoid any misunderstanding, we want to point out that the m_1 and m_3 sum rules have been evaluated using in Eqs. (3) the one-body kinetic-energy operator $-\frac{1}{2} \sum \Delta_i$.

A deeper understanding of the meaning and limitations of E_3 can be obtained by comparing Eq. (6) with the plasmon peak energy ω which can be obtained within RPA performing a q expansion (see, for example, Sec. 15 of Ref. 12). Up to the q^4 terms, we find

$$\omega^2 = \omega_p^2 + \frac{3}{5} v_F^2 q^2 + \left(\frac{1}{4} + \frac{12}{175} \frac{v_F^4}{\omega_o^2} \right) q^4. \quad (7)$$

This formula was first derived by Ferrell,¹³ although up to the q^2 term was already known after the work of Bohm and Pines.⁸

The comparison of Eq. (6) without exchange or correlation and Eq. (7) shows that $\omega \approx E_3$. Indeed, we have checked that for values of q as big as q_c , the difference between ω and E_3 is smaller than 2% for all the metals here studied.

Since $E_3 \leq \omega$ one might think at first glance that the inequalities $E_1 \leq \bar{E} \leq E_3$ are being violated. This is not quite so. Let us stress again that \bar{E} is an average over the whole spectrum, including all the electron-hole excitations and not only the collective mode, which is the only one described in an approximated way by Eq. (7). As a consequence, at high q , $E_3(q)$ goes over $q^2/2$, but not $\omega(q)$ which is strictly not valid above q_c . The $q^4/4$ term in Eq. (7) should not be interpreted as the quasi-free-electron energy. The key point is that for values of q for which the bulk plasmon is a well-defined collective excitation, E_3 is a reasonably good approximation to \bar{E} and to ω . For small q , it is reasonable that $\bar{E} < \omega$ because \bar{E} comes from an average of ω with noncollective small-energy electron-hole excitations bearing very little strength (see for illustrative purposes Fig. 1 of Ref. 13).

Expanding the square root of Eq. (6) in a q^2 series, we get the dispersion relation

$$\omega_3(q) \approx \omega_p + A_3 q^2 + B_3 q^4, \quad (8)$$

where $A_3 = \alpha_3/2\omega_p$ is the elastic q^2 dispersion coefficient and $B_3 = (1 - 4A_3^2)/8\omega_p$.

So far, we have used m_1 and m_3 to define the $E_3(q)$ [$\omega_3(q)$] average excitation energy. It has been shown^{7,14} that the m_3 sum rule (sometimes called the elastic sum rule) can be interpreted as a restoring force parameter associated with a collective motion of the system. Within the Landau theory of Fermi liquids, this motion is viewed as the collisionless propagation of a zero sound (see, for example, Sec. 16 of Ref. 12).

The sum rule m_{-1} can be obtained with ERPA precision from constrained Kohn-Sham (KS) calculations (see Refs. 7 and 14 and references therein). This sum rule is closely related to the static polarizability of the system, $\alpha = 2m_{-1}$, and allows one to define the $E_1 \equiv (m_1/m_{-1})^{1/2}$ mean excitation energy. E_1 is associ-

ated with another possible kind of collective excitation in metals in which a high-frequency collisional regime allows the relaxation of the system during the perturbation propagation. This collective motion corresponds to a vibration propagating as a first (ordinary) sound¹² whose frequency is well reproduced by a HD model⁹ or, alternatively, a constrained TF calculation.⁴⁻⁷

To work out m_{-1} we follow Refs. 4 and 6. Rather than solving the constrained KS problem, we solve the much simpler constrained TF problem:

$$\varepsilon[n] + \lambda e^{iq \cdot r} n, \quad (9)$$

where $\varepsilon[n]$ is the energy density functional used in Refs. 3-5 supplemented, for the sake of completeness, with the fourth-order gradient corrections to the TF kinetic-energy density as given in Ref. 15. λ is a constraining parameter, small enough so that the variational density n can be written as the unperturbed density n_0 plus an arbitrary function $\varphi(r)$ times λ : $n(r) = n_0 + \lambda \varphi(r)$.

Linearizing the Euler-Lagrange equation pertaining to the constrained TF problem (9) (see Ref. 4 for a thorough discussion), we get the following integro-differential equation for $\varphi(r)$:

$$-\frac{\beta}{4} \Delta \varphi + \left[\frac{1}{3} v_F^2 - \frac{v_F}{3\pi} - \xi \right] \varphi + n_0 e^{iq \cdot r} + n_0 \int d\mathbf{r}' \frac{\varphi(\mathbf{r}')}{|\mathbf{r} - \mathbf{r}'|} + \frac{1}{270} \frac{1}{v_F^2} \Delta^2 \varphi = 0. \quad (10)$$

To arrive at this equation, we have used the fact that the density n_0 of the unperturbed system is constant.

The Laplacian term in Eq. (10) arises from the second-order (\hbar^2) corrections to the TF kinetic-energy density, and the bi-Laplacian term for the fourth-order (\hbar^4) corrections. We shall use the exact value of the so-called Weizsäcker coefficients,¹⁵ $\beta = \frac{1}{9}$, although other values are also currently employed (see, for instance, Refs. 3 and 4 and references therein). ξ has been defined in Eq. (5).

Equation (10) can be analytically solved using standard Fourier transform techniques. We get

$$\varphi(r) = \frac{-n_0 q^2 e^{iq \cdot r}}{\omega_p^2 + \left[\frac{1}{3} v_F^2 - \frac{v_F}{3\pi} - \xi \right] q^2 + \frac{\beta}{4} q^4 + \frac{1}{270} \frac{q^6}{v_F^2}} \quad (11)$$

and^{4,5}

$$m_{-1} = -\frac{1}{2} \int d\mathbf{r} e^{iq \cdot r} \varphi^*(r).$$

Consequently, the TF static polarizability per electron is

$$\frac{2m_{-1}}{N} = \frac{q^2}{\omega_p^2 + \left[\frac{1}{3} v_F^2 - \frac{v_F}{3\pi} - \xi \right] q^2 + \frac{\beta}{4} q^4 + \frac{1}{270} \frac{q^6}{v_F^2}}. \quad (12)$$

To our knowledge, Eq. (12) has not been previously discussed in the literature. Although it has been obtained

from a TF (i.e., HD) calculation, it is a good approximation to the ERPA value. That may be easily shown in the case of a free electron gas, for which the exact polarizability per electron can be obtained as¹²

$$\frac{\alpha}{N} = \frac{2m_{-1}}{N} = \frac{3}{v_F^2} \left[1 - \frac{1}{x} \left[1 - \frac{x^2}{4} \right] \ln \left[\frac{1-x/2}{1+x/2} \right] \right], \quad (13)$$

where $x \equiv q/q_F$. Setting to zero all the terms coming from the Coulomb interaction, we obtain the free-electron limit of Eq. (12):

$$\frac{\alpha}{N} = \frac{2m_{-1}}{N} = \frac{1}{\frac{1}{3} v_F^2 + \frac{\beta}{4} q^2 + \frac{1}{270} \frac{q^4}{v_F^2}}. \quad (14)$$

Each term in the denominator of Eq. (14) has a clear origin. The first one comes from the standard TF kinetic energy, the q^2 term from the second-order (\hbar^2) gradient correction to it, and the q^4 term from the fourth-order (\hbar^4) gradient corrections.

Figure 1 shows m_{-1}/N as a function of q/q_F ; we have used the Al v_F value ($r_s = 2.07$ a.u.). Referring to the three upper curves, the solid line is the exact result [Eq. (13)]; the dashed line includes up to the \hbar^2 corrections and the dashed-dotted one up to the \hbar^4 corrections, both obtained from Eq. (14). One can see that the agreement between the exact and TF calculations is excellent up to $q/q_F \sim 1$ (\hbar^2 TF) and up to $q/q_F \sim 1.5$ (\hbar^4 TF), well above the $q_c/q_F \sim 0.68$ value. This is not surprising, since

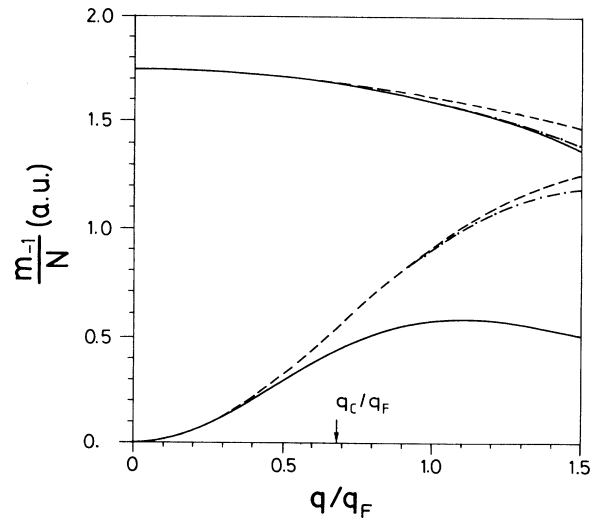


FIG. 1. m_{-1}/N for Al as a function of q/q_F . Upper curves, free-electron gas results: solid line from Refs. 6 and 12, dashed line from \hbar^2 TF and dashed-dotted line from \hbar^4 TF. Lower curves, including the interaction: dashed line from \hbar^2 TF, dashed-dotted line from \hbar^4 TF, and solid line from the results of Ref. 17.

the exact expression (13) and the TF expression (14) coincide up to order $(q/q_F)^4$.⁴ Indeed, expanding these equations in powers of x , it is easy to check that

$$\left[\frac{\alpha}{N} \right]_{\text{TF}} = \frac{3}{v_F^2} \left(1 - \frac{1}{12} x^2 - \frac{1}{240} x^4 - \dots \right) = \left[\frac{\alpha}{N} \right]_{\text{exact}}.$$

Using the order- \hbar^6 corrections to the TF kinetic-energy density as derived by Murphy,¹⁶ we have verified that the (α/N) \hbar^6 TF expression agrees with the exact result up to order x^6 .

From m_1 and m_{-1} we get

$$\begin{aligned} E_1^2 \equiv \frac{m_1}{m_{-1}} &= \omega_p^2 + \left[\frac{1}{3} v_F^2 - \frac{v_F}{3\pi} - \xi \right] q^2 + \frac{\beta}{4} q^4 + \frac{1}{270} \frac{q^6}{v_F^2} \\ &\equiv \omega_p^2 + \alpha_1 q^2 + \frac{\beta}{4} q^4 + \frac{1}{270} \frac{q^6}{v_F^2}. \end{aligned} \quad (15)$$

This expression, together with Eqs. (6) and (12), is the basic results of the present study. It is worth noting that contrary to E_3^2 and m_3 , E_1^2 and m_{-1} are q^2 expansions due to the \hbar expansion inherent to the TF kinetic-energy density. Indeed, associated with each order- \hbar^{2n} gradient correction to the TF kinetic energy, there is a q^{2n+2} term in the denominator of Eq. (12).

An equation similar to (15), using $\beta=1$ and without including exchange, correlation, or \hbar^4 terms, has been given by Penn.¹⁷ That equation would appreciably underestimate the free m_{-1}/N value. For comparison, we show in Fig. 1 (lower solid line) the complete (ω_p^2) term included m_{-1}/N result obtained using Penn's formula, as well as the interacting electron results up to orders \hbar^2 and \hbar^4 obtained from Eq. (12) (lower dashed and dashed-dotted lines, respectively).

Neglecting the q^6 term in Eq. (15) (its contribution is negligible for the q/q_F values we will be showing) and expanding the square root of this equation in powers of q^2 , we get

$$\omega_1(q) \approx \omega_p + A_1 q^2 + B_1 q^4, \quad (16)$$

where $A_1 = \alpha_1/2\omega_p$ is the hydrodynamical q^2 dispersion coefficient and $B_1 = (\beta - 4A_1^2)/8\omega_p$. It is worth noting the appearance in A_1 of the square of the first sound velocity $v_F^2/3$, whereas in A_3 appears the so-called RPA coefficient $3v_F^2/10\omega_p$.

To finish this section, we would like to point out that both average energies, E_1 and E_3 , have been used in the past to estimate the plasmon frequency of NFE metals in a variety of geometries, the former one after the work of Lushnikov and co-workers^{18,19} and the latter one after the work of Bertsch and Ekardt.^{20,21,3}

III. RESULTS

We display in Table I the experimental quantities relevant for the discussion of our results. r_s is the bulk radius per electron, $\omega(q=0)$ the plasmon energy at $q=0$, A_{SFF} the q^2 dispersion coefficient, m^* the electron effective band mass, and ϵ the static dielectric constant. m^* , $\omega(q=0)$, and A_{SFF} have been taken from Refs. 1 and

TABLE I. Experimental quantities relevant for our description of the plasmon dispersion relation. r_s , $\omega(q=0)$, and A_{SFF} are given in a.u., m^* in units of the bare electron mass, and ϵ is dimensionless.

	r_s	ϵ	m^*	$\omega(q=0)$	A_{SFF}
Al	2.07	1.05		0.551	0.30
Na	3.93	1.13	1.05 ± 0.04	0.212	0.17
K	4.86	1.21		0.140	0.075
Rb	5.20	1.29	1.25 ± 0.06	0.125	0.045
Cs	5.62	1.37		0.107	-0.18

2, the latter quantity has been obtained in these references from a fit to their $q < q_c$ experimental data. Since ϵ is not available for the metal state, it has been obtained either from the corresponding experimental ion polarizability²² using the Clausius-Mossotti relation, or from the experimental susceptibility.²³ As indicated in Ref. 2, these ϵ values are probably too high due to the way they have been determined.

Some care should be taken about which electron effective mass to consider if one wants to include band effects. We completely adhere to the point of view of SFF that m^* should be the one obtained from the study of intraband transitions. This point has been thoroughly discussed in Ref. 2.

Table II collects the results we have obtained for $\omega(q=0)$, A_1 , and A_3 using Eqs. (8) and (16). One can see that A_1 and A_3 are very different, especially for low electron density metals. This indicates that the $\omega_1(q)$ and $\omega_3(q)$ dispersion relations yield completely different results for nonzero values of q . It is also worth noting that the Cs HD dispersion coefficient A_1 is negative.

We display in Figs. 2 and 3 the results for Al and Cs. The solid lines correspond to the E_1 and E_3 energies calculated from Eqs. (15) and (6), respectively. Actually, for the range of q values displayed in these figures and in those of Refs. 1 and 2, Eqs. (8) and (16) are a very good approximation to the exact Eqs. (6) and (15). The use of other state-of-the-art representations of the local correlation energy, like those of Refs. 24 and 25, do not change the value of the q^2 coefficient in more than 1% for Al and 4% for Cs.

Also shown in the figures are the SFF experimental data (dots), the results obtained from the Lindhard-

TABLE II. Values of the plasmon energy and q^2 slopes at the origin obtained from Eqs. (8) and (16). Also shown are the Fermi velocity v_F and the ξ parameter defined in Eq. (5). All these quantities are in a.u.

	$\omega(q=0)$	A_1	A_3	v_F	$10^3 \xi$
Al	0.582	0.160	0.357	0.927	2.5
Na	0.222	0.054	0.197	0.488	3.7
K	0.162	0.0185	0.147	0.395	4.1
Rb	0.146	0.0070	0.131	0.369	4.2
Cs	0.130	-0.0065	0.113	0.342	4.3

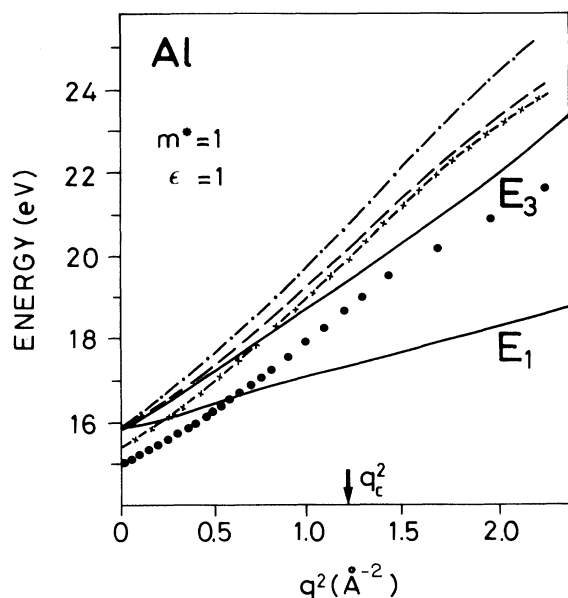


FIG. 2. Bulk-plasmon dispersion relation for Al as a function of q^2 . Circles from SFF measurements (Ref. 1); solid lines calculated from Eqs. (6) and (15); dashed-dotted line calculated from Lindhard-Mermin function; dashed line with additional inclusion of the Vashista-Singwi corrections; and crossed-dashed line with further inclusion of core polarization. The cutoff q_c^2 (arrow) has been obtained from the experimental $\omega(q=0)$ and r_s values.

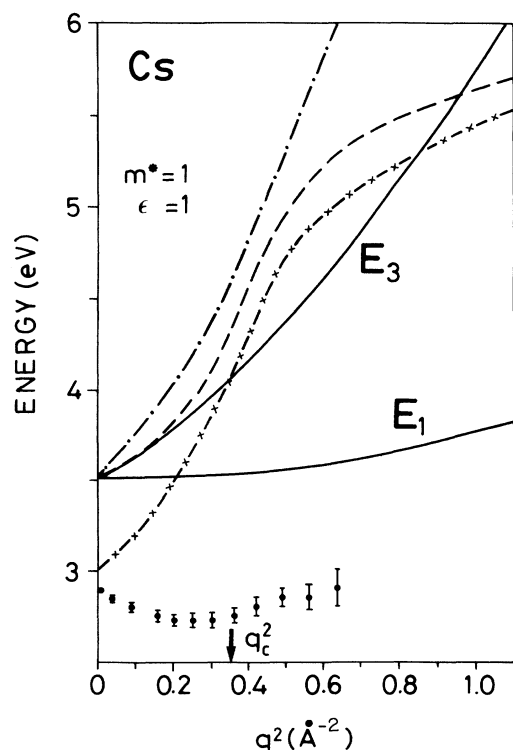


FIG. 3. Same as Fig. 2 for Cs. The experimental results have been taken from Ref. 2.

Mermin (LM) dielectric function²⁶ (dashed-dotted line), and the results from the Vashista-Singwi (VS) model,²⁷ which corrects the LM results by adding exchange and correlation effects as defined by Nozières and Pines²⁸ (dashed line); finally, the crossed-dashed line has been obtained from the VS results by further inclusion of core polarization.^{1,2} We want to indicate that these figures, as well as Figs. 4 and 5, have been obtained adding our results to the corresponding SFF figures.

Some interesting conclusions can be drawn from the inspection of Figs. 2 and 3, and from the comparison of Tables I and II. Notice that when exchange and correlation effects are taken into account, Eq. (6) reproduces the SFF results for aluminum within $\sim 6\%$ even for values of q higher than $q_c = 0.63$ a.u. SFF find for the q^2 dispersion coefficient the value $A_{\text{SFF}} = 0.30 \pm 0.01$ a.u., whereas from VS and our Eq. (6) one finds 0.357 a.u., in much better agreement with SFF than the value of 0.44 a.u. obtained using the RPA coefficient. A similar agreement between $E_3(q)$ and the experimental results is found in Na (see Tables I and II).

Had we neglected exchange and correlation energies, we would have obtained for Al $A_3 = 0.44$ and $A_1 = 0.25$ a.u. instead of the values shown in Table II. The quenching of the q^2 dispersion coefficients is mostly due to the Coulomb exchange contribution. Indeed, for all the metals we have studied the correlation contribution is

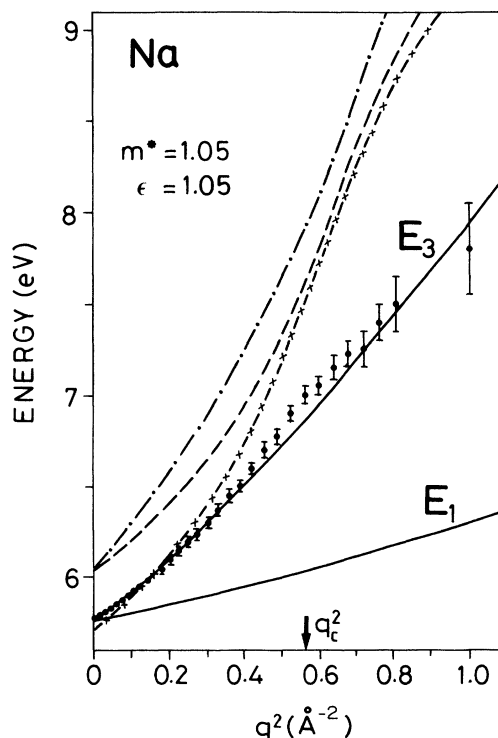


FIG. 4. Same as Fig. 3 for Na. The E_1 and E_3 curves have been obtained from Eqs. (17) and (18).

1 order of magnitude smaller.

The discrepancy between $E_3(q)$ and the experimental results for Al and Na consist in a fairly q -independent small amount. The origin of this disagreement can be attributed to atomic lattice effects, such as core-polarization and band-structure effects^{1,2,29} which are beyond the simple jellium model.

This situation is somehow close to that of the free-electron gas: $\omega(q)$ is rather well reproduced by $\omega_3(q)$, the origin of the discrepancy being traced back to atomic lattice effects. As r_s increases, the agreement between theory and experiment is gradually lost, even at $q=0$. Moreover, the experimental q^2 dispersion coefficient A_{SFF} , which was close to A_3 for Al and Na, lies now between A_1 and A_3 , and gets eventually smaller than A_1 for Cs, the only alkali metal for which we have found a negative q^2 dispersion coefficient.

Within our formalism, there is a phenomenological yet simple way of including atomic lattice effects in E_1 and E_3 . It consists in substituting the bare electron mass by m^* everywhere, and incorporating in the Coulomb energy a static dielectric constant ϵ . We obtain

$$E_1^2 = \frac{\omega_p^2}{m^* \epsilon} + \left[\frac{1}{3} \left(\frac{v_F}{m^*} \right)^2 - \left(\frac{v_F}{3\pi} + \xi \right) \frac{1}{m^* \epsilon} \right] q^2 + \left[\frac{\beta}{4} + \frac{1}{270} \frac{q^2}{v_F^2} \right] \frac{q^4}{m^{*2}} \quad (17)$$

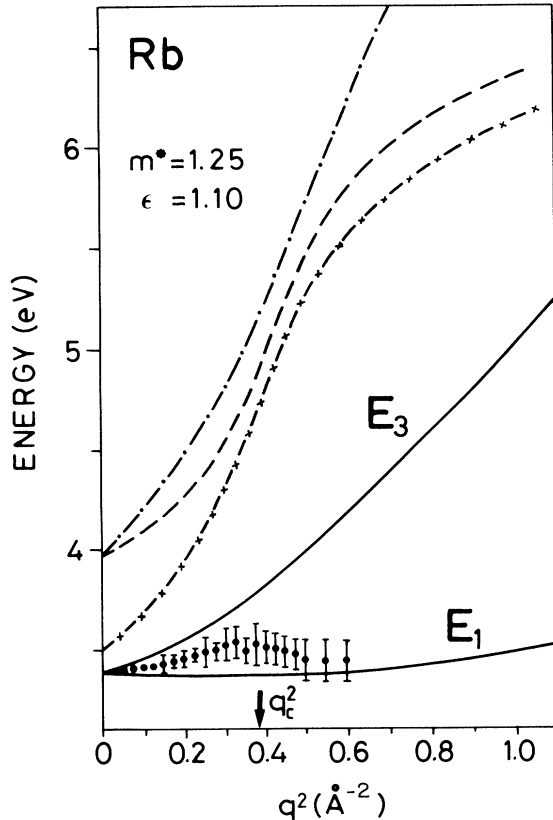


FIG. 5. Same as Fig. 4 for Rb.

and

$$E_3^2 = \frac{\omega_p^2}{m^* \epsilon} + \left[\frac{3}{5} \left(\frac{v_F}{m^*} \right)^2 - \left(\frac{v_F}{3\pi} + \xi \right) \frac{1}{m^* \epsilon} \right] q^2 + \frac{1}{4} \frac{q^4}{m^{*2}}, \quad (18)$$

where for the sake of clarity, we have kept for ω_p , v_F , and ξ the definitions given after Eq. (4), with the only change $b \rightarrow b\epsilon/m^*$.³⁰ We have considered a constant core polarization represented by ϵ . This is a valid assumption when the characteristic frequency of core-valence electron transitions is large compared with the plasmon frequency, i.e., when the core electrons are tightly bound, as is the case for alkali metals.

Equations (17) and (18) are useful if m^* and ϵ are known experimentally. Since it is partially the case only for Na and Rb, for these metals we have proceeded as follows. We have taken the experimental m^* from Ref. 2 and fixed ϵ in order to reproduce $\omega(q=0)$. This yields $\epsilon=1.05$ for Na (in good agreement with the value 1.06 estimated by Taut³¹) and 1.10 for Rb, values smaller than the ones estimated from the experimental ion polarizability (see Table I). The corresponding A_1 and A_3 are $A_1=0.0514$, $A_3=0.188$ for Na, and $A_1=-0.0120$, $A_3=0.0814$ for Rb. Still, the experimental q^2 dispersion coefficient A_{SFF} for Na is close to A_3 , whereas for Rb it lies between A_1 and A_3 . In Figs. 4 and 5 we compare our results for these metals with the ones obtained from other models and from the SFF experiments. We have used the same type of drawing as in Figs. 2 and 3.

IV. DISCUSSION AND CONCLUDING REMARKS

We have obtained two analytical dispersion relations for the bulk plasmon in NFE metals which include in a transparent way exchange and correlation effects. As compared with other methods of considering these effects, like that of VS, our expressions are more manageable. In particular, the $\omega_3(q)$ dispersion relation yields results in full agreement with these of VS for small q values (see, for example, Figs. 2 and 3), and in better agreement with experiments than theirs elsewhere.

The use of a static dielectric constant allows one to take care of core-polarization effects in an effective manner. To account for band-structure effects, we have phenomenologically included the electron effective mass. In this way, atomic lattice effects can be considered without complicating appreciably the dispersion relations.

As indicated in Sec. II, Eqs. (6) and (18) are exact results (within a LDA for exchange and correlation energies) of what should be interpreted as the upper bound of the center of gravity of the ERPA electron-energy-loss function. This bound is very close to the peak position only for plasma excitations at small q values of weakly inhomogeneous systems. When q increases, the E_3 energies contain an increasingly large electron-hole excitations contribution (very likely, the experimental peak position

is also affected at large- q values by the growing multiple-scattering background²⁹). Nevertheless, for high-density NFE metals our method seems to be a successful approach even for $q \geq q_c$, as is the case of Na (see Fig. 4).

For Al we do not have the experimental band m^* necessary to carry out the calculation. However, in Ref. 29 Sturm calculates separately the shifts of the plasmon energy at $q=0$ due to band-structure and core-polarization effects. Taking his values $(\Delta\omega_p)_{\text{band}} = -0.3$ eV and $(\Delta\omega_p)_{\text{core}} = -0.4$ eV to infer the m^* and ϵ to be used in Eq. (18), we obtain $m^* = 1.045$ and $\epsilon = 1.05$. When used in that equation, these values yield results in excellent agreement with experiment.³²

For low electron density alkali metals, correlation-induced anomalies in the plasmon dispersion appear,³³ and regions with negative dispersion coefficient show up as inhomogeneity and anisotropy effects become more important. Nevertheless, according to Taut's calculations,³³ due to their weak pseudopotential these effects are small for Na and K, less than 0.1% for all the q values displayed in the figures. For Al, the anisotropic effect is also very small, as predicted by Sturm²⁹ and confirmed experimentally in Ref. 1.

We conclude that for high-density metals like Na and

Al, E_3 as given by Eq. (18) yields results in good agreement with the experimental data. It bears the main physical ingredients needed to describe the perturbation propagation which, in a monopolar point of view, is of collective character for small q values and becomes an electron-hole excitation for large q values.

Since for small q values the anisotropy and inhomogeneity effects have little influence on the A coefficient,^{31,34} we would finally like to point out another possible explanation of the evolution of A_{SFF} with r_s that cannot be definitely ruled out. This is a gradual evolution of the response of the system from a collisionless regime for high electron density metals to a rather hydrodynamical, collisional regime for low electron density metals. This alternative explanation is prompted by the appearance of negative A_1 values for large r_s .

ACKNOWLEDGMENTS

We would like to thank G. Benesch, J. P. da Providencia, and X. Viñas for useful discussions and Miquel Canals for his help with Fig. 2. This work has been supported in part by the Dirección General de Investigación Científica y Técnica (DGICYT, Spain), Grants No. PB89.0332 and No. AE87-0027.

*Permanent address: Departament d'Estructura i Constituents de la Matèria, Facultat de Física, Universitat de Barcelona, Diagonal 647, E-08028 Barcelona, Spain.

¹J. Sprösser-Prou, A. vom Felde, and J. Fink, Phys. Rev. B **40**, 5799 (1989).

²A. vom Felde, J. Sprösser-Prou, and J. Fink, Phys. Rev. B **40**, 10 181 (1989).

³Ll. Serra, F. Garcias, M. Barranco, J. Navarro, L. C. Balbás, and A. Mañanes, Phys. Rev. B **39**, 8247 (1989).

⁴Ll. Serra, F. Garcias, M. Barranco, J. Navarro, L. C. Balbás, A. Rubio, and A. Mañanes, J. Phys. Condens. Matter **1**, 10 391 (1989).

⁵Ll. Serra, F. Garcias, M. Barranco, N. Barberán, and J. Navarro, Phys. Rev. B **41**, 3434 (1990).

⁶C. García-Recio, H. Krivine, N. Van Giai, and J. Navarro, Nucl. Phys. A **507**, 385 (1990).

⁷E. Lipparini and S. Stringari, Phys. Rep. **175**, 103 (1989).

⁸D. Pines, *Elementary Excitations in Solids* (Benjamin, New York, 1964); D. Bohm and D. Pines, Phys. Rev. **85**, 338 (1952); **92**, 609 (1953).

⁹S. Stringari, J. Low Temp. Phys. **57**, 307 (1984).

¹⁰J. Navarro and M. Barranco, Nucl. Phys. A **505**, 173 (1989); **519**, 847 (1990).

¹¹B. Goodman and A. Sjölander, Phys. Rev. B **8**, 200 (1973).

¹²A. L. Fetter and J. D. Walecka, *Quantum Theory of Many-Particle Systems* (McGraw-Hill, New York, 1971).

¹³R. A. Ferrell, Phys. Rev. **107**, 450 (1957).

¹⁴O. Bohigas, A. M. Lane, and J. Martorell, Phys. Rep. **51**, 267 (1979).

¹⁵M. Brack, C. Guet, and H. B. Håkansson, Phys. Rep. **123**, 275 (1985).

¹⁶D. R. Murphy, Phys. Rev. A **24**, 1682 (1981).

¹⁷D. R. Penn, Phys. Rev. B **13**, 5248 (1976).

¹⁸A. A. Lushchikov and A. J. Simonov, Z. Phys. **270**, 17 (1974).

¹⁹A. A. Lushchikov, V. V. Maksimenko, and A. J. Simonov, in *Electromagnetic Surface Modes*, edited by A. D. Boardman (Wiley, New York, 1982), Chap. 8.

²⁰G. Bertsch and W. Ekardt, Phys. Rev. B **32**, 7659 (1985).

²¹M. Brack, Phys. Rev. B **39**, 3533 (1989).

²²J. R. Tessmann, A. H. Kahn, and W. Shockley, Phys. Rev. **92**, 890 (1953).

²³S. E. Schnatterly, J. J. Ritsko, and J. R. Fiels, Phys. Rev. B **13**, 2451 (1976).

²⁴S. H. Vosko, L. Wilk, and M. Nusair, Can. J. Phys. **58**, 1200 (1980).

²⁵J. P. Perdew and A. Zunger, Phys. Rev. B **23**, 5048 (1981).

²⁶J. Lindhard, K. Dan. Vidensk. Selsk. Mat. Fys. Medd. **28**, 1 (1954); N. D. Mermin, Phys. Rev. B **1**, 2362 (1970).

²⁷P. Vashista and K. S. Singwi, Phys. Rev. B **6**, 875 (1972).

²⁸P. Nozières and D. Pines, Nuovo Cimento **9**, 470 (1958).

²⁹K. Sturm, Z. Phys. B **29**, 27 (1978).

³⁰We have incorporated m^* and ϵ in the exchange and correlation terms using dimensional arguments.

³¹M. Taut, J. Phys. C **19**, 6009 (1986).

³²Ll. Serra, F. Garcias, N. Barberán, M. Barranco, J. Navarro, and A. Rubio, Z. Phys. D (to be published).

³³M. Taut, Solid State Commun. **65**, 905 (1988).

³⁴K. Sturm, Solid State Commun. **27**, 645 (1978).